Precise Determination of the $2s_{1/2}$-$2p_{1/2}$ Splitting in Very Heavy Lithiumlike Ions Utilizing Dielectronic Recombination

C. Brandau,[1] C. Kozhuharov,[2] A. Müller,[1] W. Shi,[1] S. Schippers,[1] T. Bartsch,[1] S. Böhm,[1] C. Böhme,[1] A. Hoffknecht,[1] H. Knopp,[1] N. Grün,[3] W. Scheid,[3] T. Steih,[3] F. Bosch,[2] B. Franzke,[2] P. H. Mokler,[2] F. Nolden,[2] M. Steck,[2] T. Stöhlker,[2] and Z. Stachura[4]

[1]*Institut für Kernphysik, Justus-Liebig-Universität, D-35392 Giessen, Germany*
[2]*Gesellschaft für Schwerionenforschung (GSI), D-64291 Darmstadt, Germany*
[3]*Institut für Theoretische Physik, Justus-Liebig-Universität, D-35392 Giessen, Germany*
[4]*Instytut Fizyki Jądrowej, 31-342 Kraków, Poland*

(Received 19 December 2002; published 14 August 2003)

The $2s_{1/2}$-$2p_{1/2}$ energy splittings ΔE_L of the lithiumlike ions $^{197}_{79}Au^{76+}$, $^{208}_{82}Pb^{79+}$, and $^{238}_{92}U^{89+}$ have been measured at the Experimental Storage Ring, utilizing low energy dielectronic recombination. The resonance energies in total 41 different $1s^2\,2p_{1/2}nl_{j'}$ ($n \geq 20$) autoionizing Rydberg states populated in the dielectronic capture process have been determined. The $2s_{1/2} \rightarrow 2p_{1/2}$ excitation energies have been obtained by extrapolation of these resonance energies to the associated series limits $n \rightarrow \infty$. The combined analysis of the experimental data for all three ions yields $\Delta E_L = 216.134(96)$ eV for Au^{76+}, 230.650(81) eV for Pb^{79+}, and 280.516(99) eV for U^{89+}.

DOI: 10.1103/PhysRevLett.91.073202 PACS numbers: 34.80.Lx, 31.10.+z, 31.30.Jv

The spectroscopy of very heavy lithiumlike ions has been a scientific focus in the last ten years, aiming at a test of quantum electrodynamics (QED) in strong central fields. In comparison with hydrogenlike ions the experimental sensitivity allows one to probe higher order radiative corrections. Triggered by the beam-foil experiment of Schweppe *et al.* [1], who determined the $2s_{1/2}$-$2p_{1/2}$ transition energy ("Lamb shift") ΔE_L of lithiumlike uranium (U^{89+}) with an uncertainty as low as 0.1 eV, a large number of QED calculations for lithiumlike ions have been carried out (cf. [2–6]). Other experiments with very heavy lithiumlike ions have been performed for the $2s_{1/2}$-$2p_{3/2}$ energy interval at the SuperEBIT electron-beam ion trap in Livermore [7,8] providing a sensitivity to QED contributions, which is comparable to or slightly better than that of the measurement of Schweppe *et al.* [1]. However, for the $2s_{1/2}$-$2p_{1/2}$ splitting the latter remains the only precise experiment for $Z > 54$ (for $Z = 54$ see Ref. [9]). Because of the lack of experimental data for other nuclei the theoretical investigations were mainly focused on $^{238}_{92}U^{89+}$ so far. The uncertainties in the nuclear structure of ^{238}U limit the accuracy of QED calculations for this nucleus [5,10]. In this respect the doubly magic nucleus $^{208}_{82}Pb$ is a much better and, in fact, the ideal candidate for testing QED in strong fields [11] since its nuclear properties are known with exceptionally high precision [12].

In this Letter we present a series of measurements on dielectronic recombination (DR) performed with the three different lithiumlike ions $^{197}_{79}Au^{76+}$, $^{208}_{82}Pb^{79+}$, and $^{238}_{92}U^{89+}$ employing the electron cooler of the Experimental Storage Ring (ESR) in Darmstadt as a free-electron target. From a combined analysis of in total 41 (16 for Au^{76+}, 12 for Pb^{79+}, and 13 for U^{89+}) different $1s^2\,2p_{1/2}nl_{j'}$ ($n \geq 20$) DR resonance groups, the $2s_{1/2}$-$2p_{1/2}$ energy splittings for the above ions have been determined.

In contrast to conventional optical experiments which aim at a precise determination of the wavelengths of emitted or absorbed photons the spectroscopic aspects of DR cross section measurements are associated with the resonance condition for the initial radiationless dielectronic capture (DC, time-reversed autoionization) of a free electron. If — in a second step — the doubly excited intermediate state decays radiatively below the autoionization threshold, DR is completed. Correspondingly, an increased rate of recombined ions is detected at relative electron-ion energies equal to the DR resonance energies. For the $2s_{1/2} \rightarrow 2p_j$ ($j = 1/2, 3/2$) core excitations of lithiumlike ions DR can be described by

$$e^- + A^{q+}(1s^2\,2s_{1/2}) \rightarrow A^{(q-1)+}(1s^2\,2p_j nl_{j'})^{**} \rightarrow A^{(q-1)+} + \text{photons}. \quad (1)$$

The capture of the free electron proceeds into high-Rydberg states with $n \geq n_{\min}$, where $n_{\min}$ characterizes the energetically lowest autoionizing state. For all three ions $n_{\min} = 20$ for the $2s_{1/2} \rightarrow 2p_{1/2}$ excitation and $n_{\min} = 6$ (gold, lead) or $n_{\min} = 5$ (uranium) for the $2p_{3/2}$ resonances. With increasing relative energy a series of $2p_{1/2}nl'_j$ Rydberg resonances is excited (Fig. 1).

The precision of the experimental DR resonance energies decisively benefits from the merged-beam kinematics of the electron cooler/storage ring arrangement. At low collision energies large energy changes applied in the laboratory system lead to very small shifts in the center-of-mass (c.m.) frame, that thus provides high resolution and accuracy. The potential of such photon-free DR

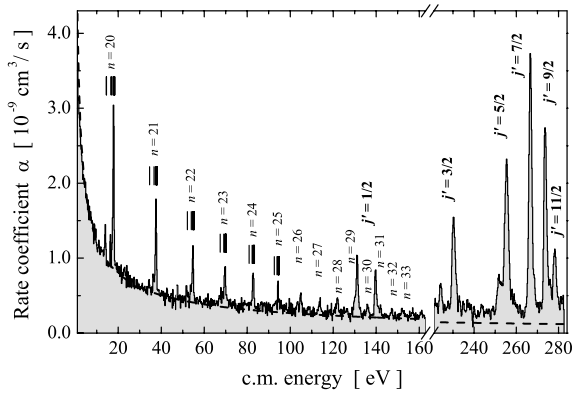

FIG. 1. Measured absolute rate coefficients α for the electron-ion recombination of Pb^{79+} in the energy range of the $1s^2\,2p_{1/2}nl_{j'}$ ($n \geq 20$) and the $1s^2\,2p_{3/2}\,6l_{j'}$ (bold labels) DR resonance groups. The $1s^2\,2p_{3/2}\,6l_{j'}$ resonances feature a fine structure splitting of about 150 eV. The individual $2p_{3/2}\,6l_{j'}$ peaks are grouped into manifolds with the same angular momentum j' and partially overlap with the weaker $2p_{1/2}nl_{j'}$ resonances. For $n = 20$–25 the calculated fine structure splitting is indicated by vertical bars. Contributions from nonresonant radiative recombination are indicated as a dashed line.

resonance studies as a highly sensitive access to QED and nuclear size contributions has already been pointed out by Spies *et al.* [13,14]. Recent examples which document the vast experimental progress during the last ten years are the DR measurements of copperlike Pb^{53+} [15] or lithiumlike F^{6+} [16]. Both ions possess resonances at very low collision energies of a few meV. Their positions were determined with an uncertainty of $\sim$1 meV. A prerequisite for such high accuracy is the existence of fortuitously low-lying single resonances preferably with a high angular momentum of the captured electron and a small (''δ-like'') natural width. Such resonances are not expected for the very heavy few-electron ions. Our approach [14] to obtain precise energies for the $2s_{1/2}$-$2p_{1/2}$ splitting is to extrapolate the resonance energies of the measured series of $1s^2\,2p_{1/2}nl_{j'}$ resonances to the series limit ($n \rightarrow \infty$) which of course is equal to the excitation energy. This novel method is of a more general nature and can in principle be applied to any excitation channel. The results are directly comparable with optically obtained transition energies and related QED calculations. Since the series limits are extracted from a multitude of resonances with well-known energy intervals this method minimizes the uncertainty of the energy calibration, utilizing the self-calibrating properties of a Rydberg series.

For our recombination studies lithiumlike ions Au^{76+}, Pb^{79+}, and U^{89+} were injected into the ESR, cooled, and stored at ion energies of about 95 MeV/u. Recombined ions were separated from the primary beam in the next dipole bending magnet downstream from the electron cooler and were detected with a plastic scintillation counter. Details of the experimental setup and of the experimental procedure can be found in [17,18]. Here we focus on the features important for a precise energy calibration. In order to change the relative energy between electrons and ions a cylindrical drift tube of 1.94 m length is mounted in the straight overlap region (2.5 m) of the two beams. Within 2 ms potentials U_d of any desired value between -5 kV and 5 kV can be applied to the drift tube, thus decelerating or accelerating the electrons. After each 30 or 40 ms dwell time interval on a given measurement potential $U_d^{(m)}$ the power supply for the tubes is switched back to its value $U_d^{(c)}$ at cooling in order to avoid ion-beam heating and changes of the ion-beam energy. A c.m.-energy range between 0 and about 100 eV can be covered with the cathode potential U_C at its value U_0 for electron cooling and by switching between grounded drift tube ($U_d^{(c)} = 0$) at electron cooling and $|U_d^{(m)}| \leq 5$ kV at measurement. Higher c.m. energies ($\lesssim$ 400 eV) were obtained increasing U_C by up to 5 kV and decelerating the electrons with the drift tube by the same amount for electron cooling. The cathode potential U_C, the drift tube voltage $U_d^{(c)}$, and the space charge potential $U_{\rm sp}^{(c)}$ at *cooling* determine the relativistic Lorentz factor $\gamma_i = (1 - \beta_i^2)^{-1/2}$ of the *ions*. Likewise the Lorentz factor γ_e of the *electrons* is given by U_C, $U_d^{(m)}$, and $U_{sp}^{(m)}$ at *measurement* potential, i.e.,

$$\gamma_{i,e} - 1 = e(U_C + U_d^{(c,m)} + U_{sp}^{(c,m)})/(m_{0,e}c^2), \qquad (2)$$

where e and $m_{0,e}$ are the charge and the rest mass of the electron, respectively, and c is the speed of light. At the experimental electron currents of 80–100 mA $U_{\rm sp} \sim$ 25 V. It lowers both, electron and ion velocity, by $\sim 2.5 \times 10^{-4}$ and is, thus, merely a small correction to the energies. An additional small shift in the ion energy — the ions are much heavier than the electrons — is introduced due to acceleration or deceleration of the ions in the drift tube. Once γ_i and γ_e are known the c.m. energy $E_{\rm c.m.}$ can easily be calculated.

The procedure to extract the series limit from the DR data consists of two steps: In the first step the energies of the $2p_{1/2}nl_{j'}$ resonance peaks are determined using the measured values for U_C, U_d, and $U_{\rm sp}$ as a preliminary energy calibration. As can be seen from Fig. 1 (and in more detail in Ref. [17]) even for the high-Rydberg states ($n \geq 20$) under investigation here the fine structure components are split by up to several eV. For $n = 20$, $j' = 1/2$ and $j' = 3/2$ are well resolved from the accumulation peak with $j' \geq 5/2$. With increasing n the splitting, the resonance strength, and the resolution are decreasing and lead to a smearing of the fine structure within one n manifold. Thus, the resonances cannot be treated as single resonances and the distribution of resonance strengths within each Rydberg manifold has to be known. In order to model the shape of the resonance groups multiconfiguration Dirac-Fock DR calculations were carried out. We

have shown previously [17] that this fully relativistic treatment provides an appropriate description if high angular momenta up to $j' = 31/2$ are included and treated on a fully relativistic basis. The theoretical cross section data for every individual $2p_{1/2}nl_{j'}$ manifold were convoluted with the experimental response function which can be represented by an anisotropic Maxwell-Boltzmann distribution [18] with parameters $k_B T_{\parallel} = 0.2$ meV and $k_B T_{\perp} = 160$ meV. The energy position of the distribution function for a n manifold of resonances is then fitted to the experimental data and all relevant experimental parameters, in particular $U_d^{(m)}$ at the position of the maximum angular momentum quantum number $j_{\max} = n - 1/2$, are stored as the reference values for the resonance energy E_{res}. For the highest angular momenta the binding energy E_B of the Rydberg electron can be described by Dirac energies in a hydrogenlike approximation [17].

The second step of the series limit determination is a global least square fit of the resonance energies according to

$$E_{\infty}(Z) = E_{\text{res}}(Z, n, j_{\max}, \gamma_i, \gamma e) + E_B(Z, n, j_{\max}). \quad (3)$$

It yields the series limits E_{∞} and, hence, the $2s_{1/2}$-$2p_{1/2}$ transition energies. The fit parameters comprise the three series limits as well as four additional energy calibration parameters. Basically, the two-step procedure can be iterated. No significant changes were found between the first and the second pass. It also has been statistically verified that the same set of calibration parameters can be used for all three ions, as expected, since the experimental conditions within the limits of reproducibility were the same for all three ions. In addition, the influence of the potential distribution of the drift tubes and the directions of the solenoidal and toroidal magnetic guiding fields in the overlap region [18] of the two beams on the resonance energies was carefully studied by means of a Monte Carlo simulation. Potential distribution and magnetic field direction in the electron-ion overlap region lead to an energy dependent shift of the individual resonances between 10 and 40 meV towards higher energies and, correspondingly to a correction for the series limits of -12 meV.

Errors of the above procedure arise from three different sources: (i) the statistical error of the fitting procedure, (ii) uncertainties in the physical model of the Rydberg resonances, and (iii) a systematical error caused by the experimental response function. Residuals of the fitting procedure of step II are displayed in Fig. 2 along with the average error $\bar{\sigma} = 30$ meV of the least square fit. In order to estimate the model uncertainties, the first step has been carried out with a pure Dirac model of the Rydberg resonances which completely neglects the mutual influence of core electrons and of the Rydberg electron on the fine structure splitting [17]. In comparison

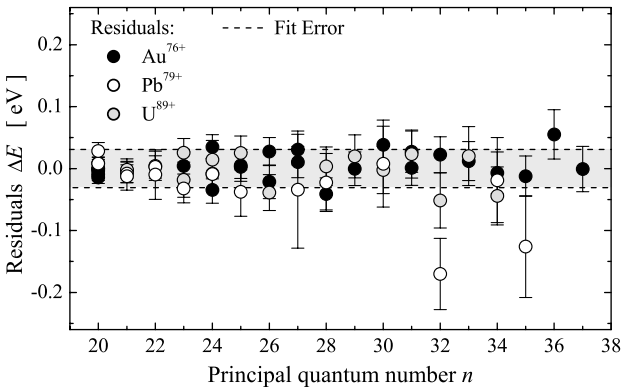

FIG. 2. Residuals of Au^{76+} (black), Pb^{79+} (white), and U^{89+} (grey) data for the global least square fit [Eq. (3)] of the $1s^2\,2p_{1/2}nl_{j'}$ resonance positions to the series limits $n \to \infty$. The error bars denote the statistical error of the peak positions. The average fit uncertainty $\bar{\sigma} = 0.03$ eV (dashed line) of the three series limits E_{∞} is provided to guide the eye. Some energy ranges were measured repeatedly yielding 57 data sets for 41 different $1s^2\,2p_{1/2}nl_{j'}$ manifolds. Please note that some of the $1s^2\,2p_{1/2}nl_{j'}$ resonance groups are blended by contributions of the $j = 3/2$ series and thus are not included in the analysis.

with the fully correlated theoretical description, deviations of the series limits of less than 28–42 meV were found depending on the ion. Additional tests with relative variations of the resonance strengths within one manifold—together with the observed agreement of measured and calculated rate coefficients within less than 10% on an absolute scale—support the finding that these deviations are an upper estimate for the model uncertainty. In contrast to $^{208}_{82}$Pb and $^{238}_{92}$U, the gold nucleus $^{197}_{79}$Au has a nonzero nuclear spin ($I = 3/2$) and magnetic moment ($\mu_I = 0.148158$). Correspondingly, the $2s_{1/2}$ state has a hyperfine splitting of 27.84 meV [19] with the $F = 1$ ground state lowered by $\Delta E(F = 1) = -16.67$ meV. Although electric and magnetic fields mainly caused by the dipole bending magnets of the storage ring can in principle lead to a repopulation of the upper hyperfine level, measurements with $^{207}Pb^{81+}$ [20] indicate that after tens of seconds of ion storage essentially all ions are in their hyperfine ground states. Therefore, for comparison with theory, which does not account for hyperfine structure, the experimental value for $E_{\infty}(^{197}_{79}Au^{76+}) = 216.151$ eV is reduced by 16.67 meV, and, in addition the model uncertainty as indicated in Table I is increased by 16.67 meV. The dominant contributions to the total systematical error of 22 meV stem from the imperfect knowledge of $kT_{\perp}$, which results in an uncertainty of 15 meV in the series limits, and of the potential distribution of the drift tube, which contributes another 15 meV. Other errors possibly arising from jitter or drift of the power supplies are at least 1 order of magnitude smaller than that and are thus negligible. Experimental results and errors for the $2s_{1/2}$-$2p_{1/2}$

TABLE I. Comparison of experimental results of this work (first three rows) for the $2s_{1/2}$-$2p_{1/2}$ transition energy in lithiumlike ions with the experimental value of Schweppe *et al.* [1] (fourth row) and with recent QED calculations [4,6]. Units are eV. The first experimental error denotes the statistical uncertainty, the second our model uncertainties, and the third the systematical errors (see text). Individual theoretical contributions are itemized in the table: finite nuclear size (fin. nucl.), nuclear recoil (nucl. rec.), one-, two-, three-photon exchange (1ph-ex, 2ph-ex, 3ph-ex respectively), self-energy and vacuum polarization (SE + VP), screening of self-energy and vacuum polarization (scr. SE + VP), and one-electron two-photon contributions (1e-2ph). The theoretical uncertainties arise from the individual errors listed in the table (first error), mainly from the nuclear size effect and three-photon exchange. For $^{238}_{92}U^{89+}$ the second error denotes uncertainties of the calculated 1e-2ph contributions. For $^{197}_{79}Au^{76+}$ and $^{208}_{82}Pb^{79+}$ calculations for 1e-2ph contributions are not available (n.a.) yet, hence the second error is an estimate for uncertaintites due to the missing graphs. For details see [4,6].

Element	Experiment	Tot. theory	Fin. nucl.	Nucl. rec.	1ph-ex	2ph-ex	3ph-ex	SE + VP	scr. SE + VP	1e-2ph
$^{197}_{79}Au^{76+}$	216.134(29)(39)(28)[a]	216.17(13)(11)[b]	−7.68(12)	−0.05	257.29(1)	−9.44	0.10(5)	−24.95	0.90	n.a.
$^{208}_{82}Pb^{79+}$	230.650(30)(22)(29)	230.68(6)(13)[b]	−10.67(2)	−0.05	278.99	−10.18	0.11(6)	−28.47	0.96	n.a.
$^{238}_{92}U^{89+}$	280.516(34)(22)(43)	280.64(11)(21)	−33.35(7)	−0.07	368.83	−13.38	0.17(8)	−42.93	1.16	0.16(21)
$^{238}_{92}U^{89+}$	280.59(10) Ref. [1]									

[a]Present experimental result has been shifted by −16.67 meV to be compared with the calculated energy which does not include the hyperfine splitting of the $2s_{1/2}$ state.
[b]Value does not include one-electron two-photon contributions.

transition energy as well as a comparison with the experimental value of Schweppe *et al.* [1] and the rigorous QED calculations of Yerokhin *et al.* [4,6] are given in Table I. For $^{238}_{92}U^{89+}$ the experimental value for the $2s_{1/2}$-$2p_{1/2}$ transition energy obtained with our photon-free technique shows good agreement with the optical value of Schweppe *et al.*, well within the error bars of both measurements. The precision of both experiments allows one to access QED contributions on a level below 0.2% of total QED, of better than 7 % of second order radiative corrections and below 3% of nuclear size effects.

Within the uncertainties we find theory and experiment to be in good agreement. With respect to the nuclear parameters the well-known doubly magic isotope $^{208}_{82}Pb$ is favorable for testing QED. Therefore, the data provided in this work will greatly help to disentangle QED and nuclear size contributions. It is interesting to see the sensitivity of the measurements to the finite size of the atomic nucleus and nuclear-physics related uncertainties in the QED calculations. DR resonances can be utilized, thus, as a probe for nuclear parameters, in particular, in relative measurements within isotopic chains.

In conclusion, we present a precise and systematic experimental study on the $2s_{1/2}$-$2p_{1/2}$ energy splitting of the three heavy lithiumlike ions Au^{76+}, Pb^{79+}, and U^{89+}. The accuracy obtained enables us to test higher order contributions of state-of-the-art calculations for QED in strong fields. For uranium our measurement provides the much needed check of the pioneering work of Schweppe *et al.* [1]. Our experimental technique provides an alternative approach to spectroscopic data and opens the door for future experiments at the border of atomic and nuclear physics.

[1] J. Schweppe *et al.* , Phys. Rev. Lett. **66**, 1434 (1991).
[2] Y.-K. Kim, D. H. Baik, P. Indelicato, and J. P. Desclaux, Phys. Rev. A **44**, 148 (1991).
[3] S. A. Blundell, Phys. Rev. A **47**, 1790 (1993).
[4] V. A. Yerokhin, A. N. Artemyev, V. M. Shabaev, M. M. Sysak, O. M. Zherebtsov, and G. Soff, Phys. Rev. A **64**, 032109 (2001).
[5] V. Shabaev, Phys. Rep. **356**, 119 (2002).
[6] V. A. Yerokhin and V. M. Shabaev, Phys. Rev. A **64**, 062507 (2001).
[7] P. Beiersdorfer, D. Knapp, R. E. Marrs, S. R. Elliott, and M. H. Chen, Phys. Rev. Lett. **71**, 3939 (1993).
[8] P. Beiersdorfer, A. L Osterheld, J. H. Scofield, J. R. Crespo López-Urrutia, and K. Widmann, Phys. Rev. Lett. **80**, 3022 (1998).
[9] D. Feili *et al.*, Phys. Rev. A **62**, 022501 (2000).
[10] T. Beier, P. J. Mohr, H. Persson, and G. Soff, Phys. Rev. A **58**, 954 (1998).
[11] G. Soff, T. Beier, M. Greiner, H. Persson, and G. Plunien, Adv. Quantum Chem. **20**, 125 (1998).
[12] G. Fricke *et al.*, At. Data Nucl. Data Tables **60**, 177 (1995).
[13] W. Spies *et al.*, Phys. Rev. Lett. **69**, 2768 (1992).
[14] W. Spies *et al.*, Nucl. Instrum. Methods Phys. Res., Sect. B **98**, 158 (1995).
[15] E. Lindroth *et al.*, Phys. Rev. Lett. **86**, 5027 (2001).
[16] M. Tokman *et al.*, Phys. Rev. A **66**, 012703 (2002).
[17] C. Brandau *et al.*, Phys. Rev. Lett. **89**, 053201 (2002).
[18] A. Hoffknecht *et al.*, Phys. Rev. A **63**, 012702 (2001).
[19] S. Boucard and P. Indelicato, Eur. Phys. J. D **8**, 59 (2000).
[20] P. Seelig *et al.*, Phys. Rev. Lett. **81**, 4824 (1998).